SAND2009-5199P

CIRCUIT MODELING TECHNIQUES APPLIED TO ZR*

P.A. Corcoran, B.A. Whitney, V.L. Bailey, I.D. Smith
L-3 Systems Pulse Sciences, San Leandro, CA 94577 USA

W.A. Stygar, M.E. Sceiford, M.E. Savage
Sandia National Laboratories, Albuquerque, NM 87185 USA

L.G. Schlitt
Leland Schlitt Consulting Services, Estes Park, CO 80517 USA

J.W. Douglas
Consultant, Oro Valley, AZ 85755 USA

Abstract

An overview of a transmission line based circuit model for the refurbished Z-machine (ZR) [1,2] is presented along with a comparison of its output to experimental measurements of ZR driving a short circuit load (Shots 1780, 1852) and a z-pinch wire load (Shot 1785, 1896). The circuit model includes a 2-D network of transmission lines that was used to model the 2-D and 3-D aspects of ZR's output transmission lines and water convolute. The development of the 2-D network is discussed along with benchmarks to a 3-D LSP-based model. The various switch parameters needed to match the measured waveshapes are also discussed.

I. BACKGROUND

The Z-machine (Fig. 1) at Sandia National Laboratory in Albuquerque, NM (SNLA) presently consists of thirty-six pulse line modules whose output currents are combined in several steps to drive centrally located loads. The individual pulse lines consist of a Marx, a coaxial Intermediate Store (IS), a coaxial Pulse Forming Line (PFL), and two vertically oriented tri-plate Output Lines (OL1, OL2). The IS, PFL, and OLs have water as their dielectric medium. The pulsed electrical power generated by each Marx is amplified as the pulse is compressed in the IS and PFL stages through successive switch closures. A Laser Triggered Gas Switch (LTGS) is located in an oil filled region at the output end of the IS and a multisite, self closing water switch is located at the output end of the PFL. Pulse front sharpening and pre-pulse suppression is accomplished through a multisite, self closing water switch at the output end of OL1, and a multisite, self closing dielectric slab switch at the end of OL2.

Pairs of pulse lines located one above the other are joined in a vertical tri-plate "mixing" region at the output end of their OL2s. The eighteen pairs of pulse line modules are arranged in a spoke like pattern every 20 degrees around the central, evacuated load region. Each of the combined OL2s then splits to drive each of the four vacuum insulator stacks in a complex 3-D structure called the water convolute (WC). The eighteen vertical tri-plate lines are thus convolved to feed the vacuum stack and the magnetically insulated transmission line (MITL) hardware which is azimuthally symmetric about the central vertical axis of the machine. Finally the four conical MITLs are joined at the Vacuum Convolute (VC) by a double post hole convolute (DPHC) where their currents are summed to drive the central load.

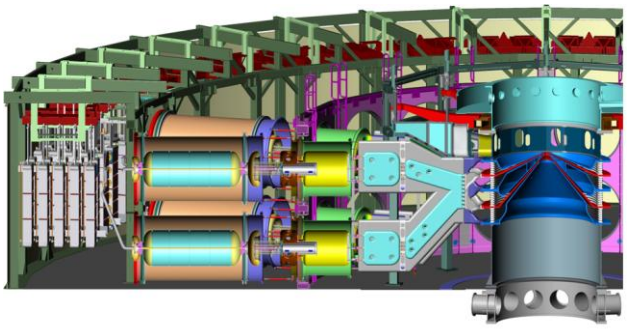

Figure 1. Cross-section of the ZR accelerator.

II. CIRCUIT TOPOLOGY AND METHODS

The ZR circuit model topology is represented by the block diagram in Fig.2. The eighteen upper pulse line modules are modeled by a single equivalent upper module, and the lower modules by a separate equivalent module. Each equivalent module produces 18 times the current of a single module in order to simulate the full

* Work was supported by Sandia National Laboratories. Sandia is a multi-program laboratory operated by Sandia Corporation, a Lockheed Martin Company, for the United States Department of Energy's National Nuclear Security Administration under contract DE-AC04-94-AL85000.

machine current in the vacuum region of the model. This circuit topology allows the effect of timing differences between the upper and lower modules to be simulated, but it implicitly models identical and simultaneous operation of the all of the modules that are represented by each equivalent. Expanded topologies are needed to accurately simulate ZR operation when there are significant timing differences between adjacent pairs of modules (e.g. when there is large switch jitter, faulty operation, or timing delays to achieve alternate pulse shapes.)

Each element in the block diagram represents a subcircuit whose dimensionality is also indicated in Fig.2. The appropriate dimension for each part of the circuit was determined by considering the local pulse time scale and geometric transit times. The ZR circuit model is zero-dimensional (0-D) in the Marx, one dimensional (1-D) in the IS through OL1, two-dimensional (2-D) in the OL2 and WC, and then back to 1-D for the Stack, MITLs, VC, and load. In this context, the model dimension refers to the degree to which physical transit times through the Z hardware are explicitly modeled by the subcircuits. 0-D circuits have no intrinsic transit times, 1-D circuits model physical transit times in only one direction, and 2-D circuits model transit times in two orthogonal directions simultaneously. The distinction between these types of circuits will be made clearer when these models are discussed in Section III.

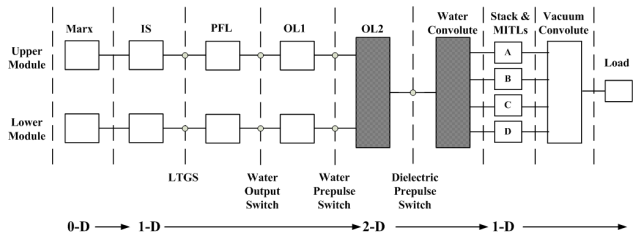

Figure 2. Block diagram showing the circuit topology.

The ZR circuit was modeled using transmission lines and resistors as the fundamental circuit elements within L-3's proprietary TLCODE software [3]. Complex multidimensional structures can be modeled in TLCODE by creating networks of orthogonal transmission lines in which each transmission line element conducts one component of the electro-magnetic (EM) pulses propagating through it. The 2-D modeling technique was developed independently at L-3 Pulse Sciences about 20 years ago for both planar and axisymmetric geometries. The 3-D technique within TLCODE was based on the Transmission Line Matrix (TLM) method [4]. Circuit models of whole accelerators such as the ZR circuit may thus contain combinations of 1-D, 2-D, and 3-D structures as may be required by the local geometry and pulse characteristics, without the usual complexities associated with interfaces between different types of solution algorithms or between separate computer software applications.

Even with automated mesh generation within the TLCODE and its rapid and inherently stable algebraic solution algorithm, there is still a strong incentive to minimize the dimension of each part of the circuit model because higher dimensioned models take longer to solve, are more complex and time consuming to set up, debug, and maintain, and are more difficult and time consuming to probe, visualize, check and understand the results of. So naturally, an effort was made at the outset to determine the least dimension that was justifiable for each section of ZR; the result was shown in Fig.2.

III. SUBSYSTEM MODELS

A. Pulseline Modules

The pulseline module model begins with the fully erected Marx generator; a DC charged capacitor, an inductor, and a series and shunt resistor. The capacitance was derived from the manufacturer's measurements and the shunt resistance is the net combination of the charge and trigger resistors. The inductance was estimated from fitting the simulated period to Marx-IS rollover waveforms from ZR Shot 6673. The series resistance was estimated from fitting the amplitude of the IS waveforms on 6673 and down line shot 1896. Due to the relatively long time scale of the IS charge time, the Marx through IS circuit could be modeled equally well using only 0-D (lumped) elements for the rollover simulations but required 1-D transmission line elements with finite transit times for the IS and its connection to the Marx when the IS begins to discharge downstream. As noted in Fig.2, the balance of the pulseline through OL1 was also modeled using 1-D transmission line elements.

The 1-D transmission line circuits were derived from hardware drawings and material properties. Mechanical drawing cross sections such as the LTGS region in Fig..3 were divided into segments that were each modeled by a single transmission line element. Voltage and current probes within the model were placed between elements at places that correspond to the probe's physical location within ZR so that direct comparisons with the data could be made. Each element's impedance (Z) and transit time (tau) were determined from the corresponding segment's inductance (L) and capacitance (C). The L and C were calculated statically using analytic formulas and computer based applications. Conduction losses in water filled regions were modeled by shunt resistors. The resulting 1-D circuit models may contain branches of 1-D elements to simulate separate current paths as required by the hardware geometry. While these branches may be viewed as quasi-2-D, the 1-D circuits have distinctly different properties from the truly 2-D circuits described in Section III-B. The 1-D topology that was developed for the LTGS region is shown in Fig. 4 beginning with the upstream plastic diaphragm and ending with the downstream diaphragm. Axially oriented transmission

lines model the oil filled volumes between the inner and outer conductors upstream and downstream of the switch. The three radial transmission line elements (above the time varying switch arc resistance) model the region that couples the upstream and downstream portions of the inner conductor; both L and C. The switch's arc inductance is modeled by the shorted stub under the arc resistor.

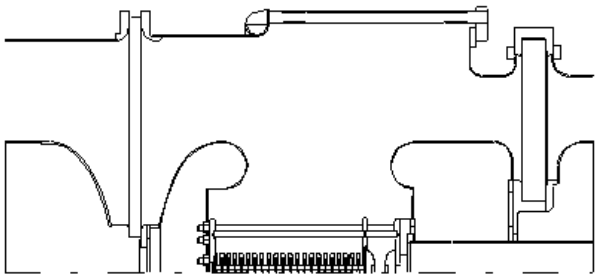

Figure 3. Cross-section of the oil-filled LTGS region.

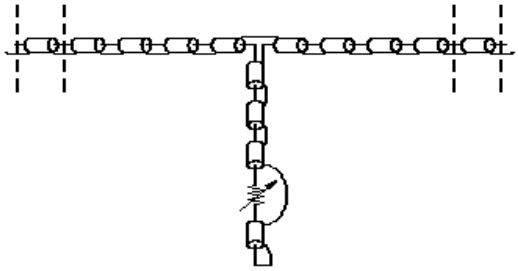

Figure 4. One dimensional transmission line model of the LTGS region. Diaphragm elements are indicated between dashed lines.

The switch loss models that control the time varying arc resistors were based measurements acquired on the HYDRUS prototype PFL gas switch [5] and the PITHON water switches [6]. These models use either a single or double exponential function for the initial "resistive phase" which settles to a constant value for the conduction phase.

B. OL2 and Water Convolute

The water filled, vertical tri-plate geometry of OL2 has large transverse transit times in order operate at high voltage while maintaining low impedance. Each cathode leg (shown in Fig. 5 where the front anode plate has been removed) is 23 inches wide with an effective width of ~34 inches when the 11 inch AK gaps are included. The transverse transit time is ~26ns in each leg and ~43ns in the mixing region downstream. These transit times are similar to the ~25ns risetime and ~100ns duration of the voltage pulse in this region. The transverse modes may be excited by the steep angle at the OL1 switches on the lower leg, timing differences between the upper and lower modules, and a relatively small number of channels at the dielectric prepulse switch. The timing differences between the upper and lower modules can be the result of switch jitter, faults in the pulseline system, and/or preset delays to affect load current pulse shaping. A simply branched 1-D model such as those used in the pulseline model will not be accurate when the transverse modes are excited, so a fully 2-D model was created.

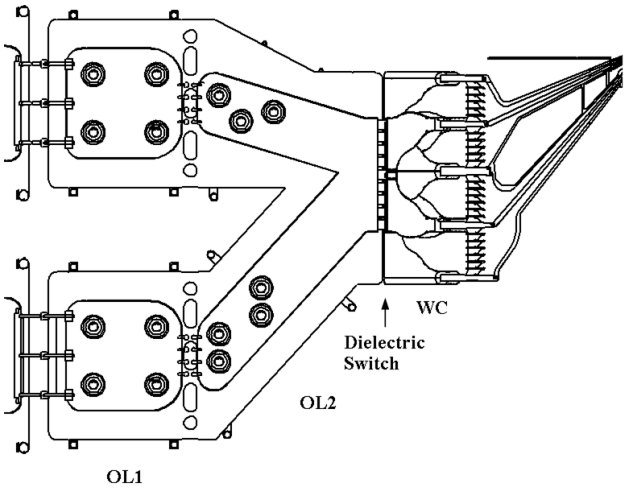

Figure 5. Cross-section of the water-filled tri-plate and convolute region outside of the vacuum stack.

The 2-D model of OL2 consists of an orthogonal mesh of 1-D transmission line elements joined periodically at four-way parallel junctions as illustrated by the sample circuit in Fig. 6. Boundary conditions are typically imposed on the transmission line fringes e.g. the voltage source, open circuit, and resistive terminations illustrated. Shunt resistors at each junction model water conduction (not illustrated). Wave propagation through the 2-D mesh behaves more or less like an L-C ladder depending on the direction of propagation rather than simply delayed by the transmission line elements. The unit mesh size between junctions (√LC transit time) must therefore be made small enough to avoid distortion caused by the excitation of the mesh units; 0.84ns was used for the OL2 mesh.

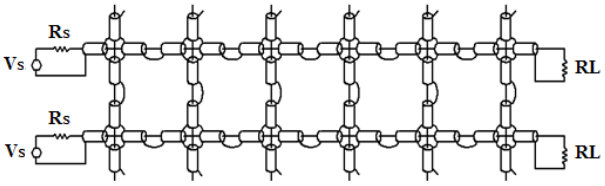

Figure 6. Typical two dimensional, shunt connected transmission line mesh.

The boundary of the mesh was set by calculating the extent of the fringing field using a 2-D electrostatic plot of the tri-plate edge cross section. The resulting boundary of the 2-D mesh is effectively 7 inches wider than the

outer boundary of the cathode, Fig 7, and extends lengthwise from the center-plane of the OL1 switches through to the tri-plate split at the entrance to the WC. The resulting fabric of transmission lines filling that boundary is illustrated in Fig. 8. A single mesh was used to model all 18 tri-plates by using 1/36 of the mesh impedance calculated for one side of the tri-plate line. A joint in the mesh was placed at the position of the dielectric switch (Fig.5) where switch elements are inserted for those shots that have dielectric slabs inserted.

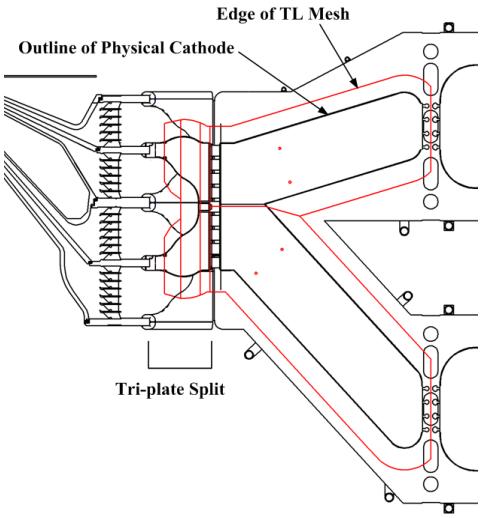

Figure 7. Boundary of the 2-D transmission line mesh (red), compared with the hardware cross-section (black).

The balance of the water convolute downstream of the split was modeled using 1-D transmissions as suggested by Fig.8 because the geometric transit times in that region are small compared to the pulse parameters even though the geometry is complex and fully 3-D. The local capacitance of each section was calculated electrostatically using 2-D cross sections through the WC and the inductance was derived through fitting to a fully 3-D electrodynamic model simulation using LSP [7]. A dynamic calculation was used instead of static because the inductance of each branch of the WC depends to some extent on the current partition and therefore the unequal inductances of the stack, MITL, VC on each level downstream.

Three separate, fully 3-D models based in LSP were used to validate the 1-D and 2-D TLCODE based models for OL2 through vacuum stack regions since there are only limited diagnostics within the OL2 portion of ZR. In each case, identical geometries were modeled in each code. The models were tested with various drive conditions using a stepped input pulse with a 1-cosine leading edge. The input rise times to peak were varied from 10ns to 100ns and different combinations of upper and lower drives were used; upper and lower together, upper only, and lower only. The non-uniform voltages and currents in the TLCODE simulations were found to match LSP's at equivalent probe positions for 10-90% risetimes of ~25ns or greater. A simple 1-D transmission line model of course could not be expected to reproduce transverse variations, but also failed to accurately match the coupling between the upper and lower legs.

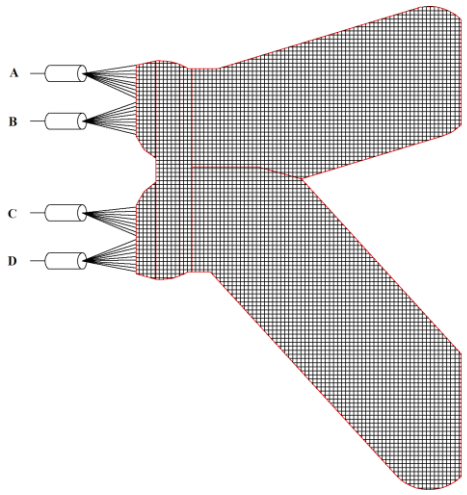

Figure 8. 2-D transmission line mesh of OL2 and tri-plate split connected to the 1-D transmission lines that model the water convolute.

The first LSP model consisted of OL2 coupled to a long, constant impedance extension of the tri-plate mixing region. This model was used to validate the 2-D transmission line model of OL2. The second LSP model consisted of OL2, WC, the vacuum stack, MITL stubs, and inductive terminations as illustrated in Fig 9. This model was used to determine the WC inductance and to validate the TLCODE model for several drive conditions. The third LSP model extended the geometry modeled in the second model to include 1.5 tri-plate lines, a 30 degree slice of ZR. This model was used to determine the coupling between adjacent OL2 lines for future extensions of the circuit that model separate OL2s as is needed for detailed pulse shape calculations.

C. Vacuum Stack, MITL, and Load

The vacuum region model begins at the water flare just outside the vacuum insulator stack with four separate chains of series connected, 1-D transmission lines. Each of those chains represents a stack/MITL level referred to as A, B, C, D and are each driven a separate branch of the WC model described in section III-C. The four levels are joined together through three, three-way parallel "tee'" connections in the model of the DPHC. The final feed geometry depends on the particular load that is fielded. To date, models have been created for the short circuit load of Shot 1780, and wire array, z-pinch loads of Shots 1785 and 1896. The vacuum region model includes shunt loss models for un-insulated vacuum electron flow and the insulated flow lost in the vacuum convolute that include the effect of cathode plasma closure [8]; and series loss models for the dynamic surface resistivity in

the MITL and final feed conductors [9]. The vacuum region model is similar to prior models that were benchmarked to Saturn and Z performance [10,11].

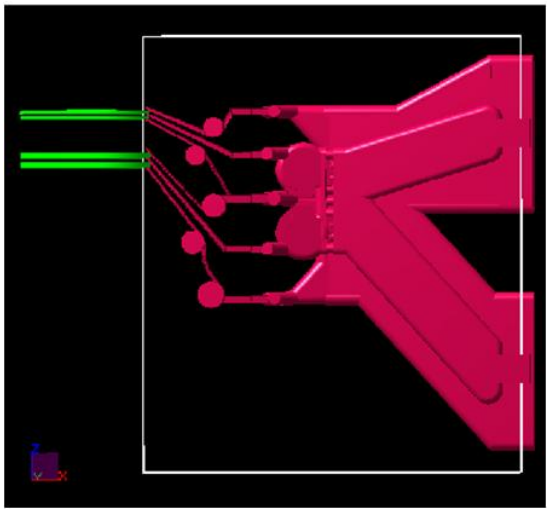

Figure 9. 3-D LSP model of the water-filled OL2, convolute, vacuum stack, and MITL stubs.

IV. VALIDATION WITH DATA

The circuit model was validated by comparing its simulated waveforms to measurements of ZR driving short circuit loads on shots 1780 and 1852 and z-pinch wire array loads on shots 1785 and 1896. In each case, the vacuum region model was altered to reflect the load that was fielded. For all but shot 1852, only the final feed and load region model was changed. For 1852, the MITL and VC models were replaced by lossless inductive stubs that modeled the large gap, flat plate, shorted radial transmission line load that was placed on each vacuum stack for cross calibrating the stack current and voltage probes. The experimentally measured Marx charge voltage and the separate IS and tank water resistivities were set as initial conditions in the simulations. Switch closure times were determined by fitting the simulation to the measured waveforms while the physical gap settings were used to determine switch inductance and the magnitude of the resistive arc losses.

The comparison of the simulations to shot data shows good general agreement of pulse shapes throughout the machine and that the model is able to produce many of the detailed waveform features on the experimental traces. Amplitudes match to within 10% depending on position and are within 2% on the vacuum region monitors, Fig. 10, 11. Simulated traces were compared to waveforms from a single module rather than the average of 18 modules because the model's topology prevents modeling the jitter between the 18 pairs of modules (Section III).

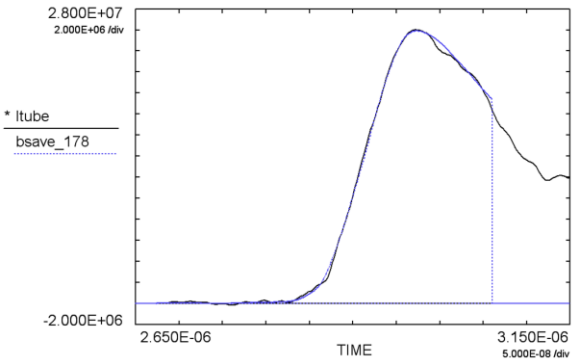

Figure 10. Simulated stack current (black) compared to experiment (blue, shot 1780).

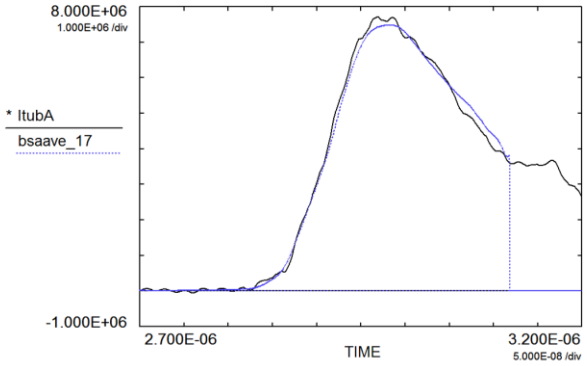

Figure 11. Simulated stack current on Level A (black) compared to experiment (blue, shot 1780).

The largest amplitude discrepancy between data and simulation appears on the PFL voltage Fig. 12; however the experimental PFL pulse amplitude varies inconsistently from module to module with both the IS and the OL1 experimental amplitudes which suggests that the PFL diagnostic's measurements are not correct. The simulated IS and OL1 amplitudes agree with the measured to within 2%, Fig. 13, 14. Improvements to the quality of the experimental measurements on more the more recent shots has produced better agreement with the simulations. Ongoing efforts at SNL and L-3 are working to resolve the remaining differences.

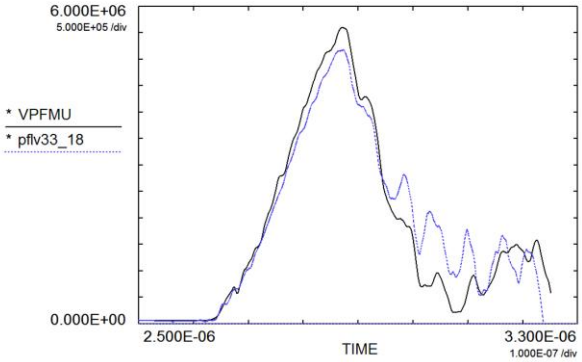

Figure 12. Simulated PFL voltage (black) compared to experiment (blue, shot 1896).

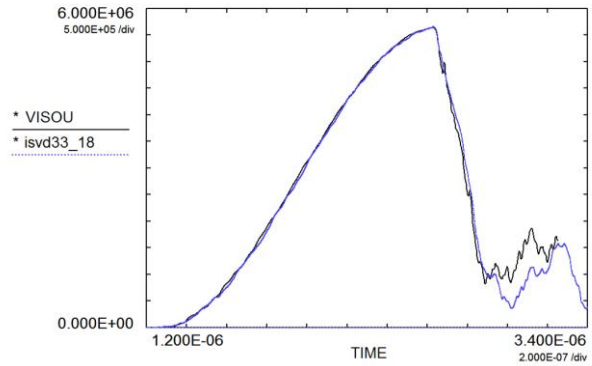

Figure 13. Simulated IS voltage (black) compared to experiment (blue, shot 1896).

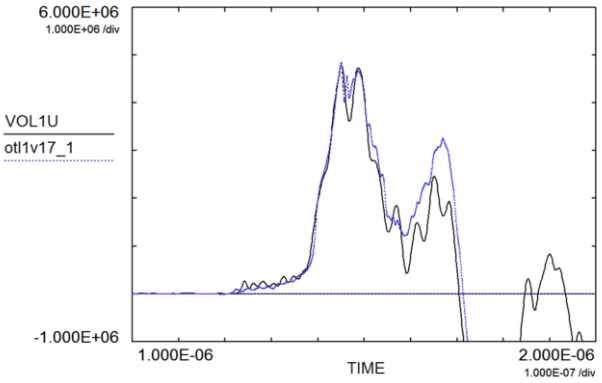

Figure 14. Simulated OL1 voltage (black) compared to experiment (blue, shot 1780).

V. CONCLUSION

The transmission line based circuit modeling techniques were applied to a model of ZR. That model consisted of circuits that explicitly model 0-D, 1-D, and 2-D wave propagation through the ZR hardware geometry. Portions of this model were validated by comparing its simulated waveform outputs to 3-D EM simulations of the OL2, WC, and vacuum region. The entire model was validated by comparing with ZR shot data on IS rollover shot 6673, short circuit load shots 1780 and 1852, and z-pinch wire array shots 1785 and 1896 where agreement to module waveforms was generally within 10% at locations with the largest discrepancies and within 2% at other locations. The model has shown to be a useful tool for understanding ZR operation and work is continuing to resolve the remaining differences between the model and experimental measurements. The ZR model topology has been expanded from what is described in this paper so that it can explicitly model six module pairs for jitter and pulse shaping simulations; the expanded model results will be described in a future publication.

VI. REFERENCES

[1] E.A. Weinbrecht, et. al., "The Z Refurbishment Project (ZR) at Sandia National Laboratories," in Proc. of the 14th IEEE Int. Pulsed Power Conf., 2003, p. 157.

[2] M.E. Savage, et. al., "An Overview of Pulse Compression and Power Flow in the Upgraded Z Pulsed Power Driver," in Proc. of the 16th IEEE Int. Pulsed Power Conf., 2007, p. 979

[3] W. N. Weseloh, "TLCODE – A Transmission Line Code for Pulsed Power Design," in Proc. of the 7th IEEE Int. Pulsed Power Conf., 1989, p. 989.

[4] P.B. Johns, "A symmetrical condensed node for the TLM method," IEEE Trans. on Microwave Theory and Tech., vol. 35, no. 4, 1987, p. 370.

[5] P.A. Corcoran, et al., "Design of an Induction Voltage Adder Based on Gas-Switched Pulse Forming Lines," in Proc. of the 15th IEEE Int. Pulsed Power Conf., 2005, p. 308.

[6] P.A. Corcoran, et al., "Pithon Experiments," presented at the HV Water Switch Workshop at Sandia National Laboratory, Albuquerque, NM., February 26, 2002.

[7] LSP is a software product developed by ATK Mission Research, Albuquerque, NM 87110, with initial support from the Department of Energy SBIR Program.

[8] W.A. Stygar, et al., "Analytic Model of a Magnetically Insulated Transmission Line with Collisional Flow Electrons," in Phys. Rev. ST Accel. Beams, 9, 090401 (2006).

[9] W.A. Stygar, et al., "Energy Loss to Conductors Operated at Lineal Current Densities ≤ 10 MA/cm: Semianalytic Model, Magnetohydrodynamic Simulations, and Experiment," Phys. Rev. ST Accel. Beams, 11, 120401 (2008).

[10] P.A. Corcoran, et. al., "PBFA-Z Vacuum Section Design Using TLCODE Simulations," in Proc. of the 11th IEEE Int. Pulsed Power Conf., 1997, p. 466.

[11] W.A. Stygar, et al., "System of Magnetically Insulated Transmission Lines that Operate at 20MA, 3MV, and 50TW: Design, Performance, and Simulations," Phys. Rev. ST Accel. Beams, pending.